A systematic study of spin-dependent recombination in GaAs1-xNx as a function of nitrogen content

Agatha Ulibarri, Rishabh Kothari, Alejandro Garcia, Jean-Christophe Harmand, Sangjun Park, Fabian Cadiz, Yves Lassailly, Jacques Peretti, Alistair Rowe

A systematic study of spin-dependent recombination in $GaAs_{1-x}N_x$ as a function of nitrogen content

Agatha Ulibarri Rishabh Kothari Alejandro Garcia Jean-Christophe Harmand Sangjun Park Fabian Cadiz Yves Lassailly Jacques Peretti Alistair Rowe**

A. C. Ulibarri, R. Kothari, A. Garcia, S. Park, F. Cadiz, Y. Lassailly, J. Peretti, A. C. H. Rowe
Laboratoire de Physique de la Matière Condensée, Ecole Polytechnique, CNRS, IP Paris, Palaiseau, 91128 France
Email Address: agatha.ulibarri@polytechnique.edu, alistair.rowe@polytechnique.edu
J. C. Harmand
Centre de Nanosciences et de Nanotechnologies, CNRS, Université Paris-Saclay, Palaiseau, 91120 France

Keywords: *spintronics, III-V semiconductors, photoluminescence, Raman spectroscopy, spin-dependent recombination, dilute nitrides*

A systematic study of spin-dependent recombination (SDR) under steady-state optical pumping conditions as a function of nitrogen content, x, in dilute nitride alloys of the form $GaAs_{1-x}N_x$ is reported. The use of very high excitation power densities up to $\approx 10^7$ Wcm^{-2} enables the full SDR versus power curves to be measured, even at relatively high nitrogen contents of $x = 0.039$. The alloy content for $0.022 \leq x \leq 0.039$ is determined to within a typical $\delta x = \pm 0.005$ by a fit of the photoluminescence (PL) spectrum using a Roosbroeck-Shockley relation which is shown to be consistent with the value obtained by studying the intensity of the GaN-like LO_2 Raman mode. PL spectra exhibit an intensity increase by a factor known as the SDR ratio when switching from a linearly- to a circularly-polarized pump. This factor reaches 5 for $x = 0.022$. The observed SDR ratio monotonically decreases with increasing x, falling to 1.5 for $x = 0.039$. Moreover, the excitation power required to obtain maximum SDR systematically increases with increasing x, varying from 0.6 mW for $x = 0.022$ to 15 mW for $x = 0.039$. These observations are consistent with an increase in the density of electronically active defects with increasing nitrogen content, both those responsible for the SDR as well as other, standard Shockley-Read-Hall centers. The result demonstrates the importance of including non-spin-dependent recombination channels in a complete model of SDR.

1 Introduction

The recombination dynamics of minority carriers in non-magnetic semiconductors become spin-dependent in the presence of a Shockley-Read-Hall (SRH) process occurring at a paramagnetic recombination center [1] due to the exchange interaction operating on quantum correlated electron pairs formed during the electron capture process. [2] If the spin-dependent recombination (SDR) rate via this route is faster than other SRH rates or the radiative band-to-band rate, luminescence and photo-current intensities can increase spectacularly when conduction electrons are spin-polarized. [2, 3] The ratio of these intensities is known as the SDR ratio.

The discovery of SDR, was initially achieved using resonance methods in crystalline [4] and amorphous [5] silicon. In direct gap III-V semiconductors, optical orientation with circularly polarized photons provides an efficient means to spin polarize conduction electrons, and SDR effects in the PL were initially observed in ternary AlGaAs alloys. [3] After a long hiatus, giant effects under optical orientation conditions were observed in dilute nitrides of the form $GaAs_{1-x}N_x$ [6, 7] where typically, $x < 0.05$. Indeed, the SDR in dilute nitrides is so large that its measurement via photoconductivity [8] has catalyzed device propositions ranging from spin filters [9] to spin-photon interfaces [10] and quantum sensors acting as light helicity detectors. [11]

In parallel with efforts to develop device applications, significant fundamental progress in the identification of the SDR-active defect in these alloys has been made. In particular, the spin dynamics of the paramagnetic center were studied, [12] and optically-detected magnetic resonance experiments have identified a Ga^{2+} interstitial defect [9, 13] as being responsible for SDR. The basic physical picture that describes SDR is now widely accepted – spin polarization of conduction electrons results in a dynamic polarization of paramagnetic centers that effectively quenches a spin-dependent SRH recombination path. This results in an overall increase in the minority-carrier lifetime which increases PL intensity occurring

via spin-independent radiative transitions. Here, we report a systematic study of the steady-state SDR at room temperature and under optical pumping conditions using a $h\nu = 1.39$ eV excitation in $GaAs_{1-x}N_x$ as a function of alloy content x and excitation power. The alloy content is estimated by fitting PL spectra with a two-component Roosbroeck-Shockley model [14] that accounts for the strain-induced splitting of the heavy- and light-hole bands, and the resulting findings are validated using an independent approach based on an intensity measurement of GaN-like LO_2 phonon mode intensities. [15] The observed variations with x in the SDR ratio and the power at which maximum SDR is measured, P_{max}, clearly indicate that the physical description of SDR must also include non-spin-dependent recombination channels. [16]

2 Determination of alloy content

A 50 nm thick p-type silicon doped, p $= 2 \times 10^{18}$ cm^{-3}, $GaAs_{1-x}N_x$ layer with a nominal $x = 0.021$ was grown on a (001) semi-insulating GaAs substrate using molecular beam epitaxy and terminated with a 10 nm GaAs cap layer. The nitrogen content, x, was found to vary significantly across the surface as optical measurements at the six points in **Figure 1(a)** will show. The normalized, room-temperature PL spectra shown in **Figure 1(b)** were obtained from a region of the sample several hundred microns across using a pump beam at 1.39 eV focused to a Gaussian spot with a lateral extent of $\sigma = 0.6$ μm. These spectra were taken at the points on the sample surface marked by the 20 x 20 μm correspondingly colored squares shown in Figure 1(a). A curved feature on the sample surface delimits the zone where a significant red shift in the PL spectrum occurs before the disappearance of the $GaAs_{1-x}N_x$ PL peak at the black measurement spot. This red shift can be due to a combination of increasing layer strain and an increase in the local nitrogen content, [17] the details of which are now analyzed via a fit to the PL lineshape.
When grown on a GaAs substrate, thin dilute nitride layers experience an in-plane bi-axial tensile strain, and an out-of-plane uni-axial compressive strain, both of which increase with increasing x. [18] Gap changes with alloy content are then described by a band-anticrossing model [17] corrected for both the hydrostatic and shear components of the in-built strain. [19] In addition to this, the shear component of the strain also splits the heavy- and light-hole degeneracy according to

$$\delta = 2 \cdot b(\epsilon_{\parallel} - \epsilon_{\perp}), \tag{1}$$

where $\epsilon_{\parallel}$ is the in-plane bi-axial strain and $\epsilon_{\perp}$ is the out-of-plane uni-axial strain. The coefficient b is the shear deformation potential of the dilute nitride.
In order to establish the nitrogen content of the five alloys studied here, the values of the heavy- and light-hole bandgaps (and therefore the hole splitting energies) were obtained by fitting the PL spectra using a Roosbroeck-Shockley relation [14] described by

$$I(h\nu) \propto [h\nu]^2\{1 - \exp[\alpha(h\nu)d]\} \exp[-h\nu/k_BT_c], \tag{2}$$

where d is the active layer thickness, $h\nu$ is the photon energy, $\alpha(h\nu)$ is the energy-dependent absorption coefficient, and k_BT_c is the carrier thermal energy. The absorption coefficient depends on the electronic density of states which, using Ullrich's approach, [14] switches smoothly from an Urbach tail at low energies to the 3D Bloch density-of-states at a critical energy, E_{cr}. E_{cr} is a fitting parameter related to the energy gap, E_g, and the width of the Urbach tail, Σ, according to $E_{cr} = E_g + k_BT_l/\Sigma$ where k_BT_l is the lattice thermal energy. The PL fits contain five parameters: Σ, k_BT_c, k_BT_l, E_{cr} and a parameter A appearing in $\alpha(h\nu)$ [14] which does not significantly change the fitting result. **Figure 2** shows an example of the strain-split light- and heavy-hole component peaks in gray and green, as well as their sum (in black) which was fit to the measured PL spectrum (in blue). E_{cr} is shown for each of the component peaks as a dotted, vertical line, while E_g associated with each of the two transitions are shown as solid vertical lines. The hole splitting, δ, obtained by taking the difference between E_g for each of the component curves, is also indicated in Figure 2. The fits are sensitive to the gap values and therefore δ can be obtained with good accuracy, typically to within a standard error of 2 meV. This is indicated by the

vertical error bars on the points in **Figure 3** and this is important to keep in mind for the following discussion on the accuracy with which it is possible to determine the alloy content, x, from these fits.
Using these obtained values of the heavy- and light-hole gaps it is possible to estimate the nitrogen content, either by using the absolute values of the gaps or by using the splitting between the two. The first approach requires the use of five parameters: two empirical band coupling parameters (V_{lh}) and V_{hh}) that appear in the anti-crossing model, [17] the hydrostatic deformation potentials for the valence (a_v) and conduction (a_c) bands, and the aforementioned shear deformation potential, b. [19] The second approach, on the other hand, only requires the use of a single empirical parameter, b, and is therefore favored here.
In the thin layer limit of relevance here, the in-plane lattice parameter of the dilute nitride is equal to the lattice parameter of the GaAs substrate, $a_{\parallel} = a_{GaAs} = 0.56535$ nm. The known, empirical dependence of the strain-relaxed lattice parameter, a, of dilute nitrides as a function of x [18] was used to calculate the in-plane bi-axial strain $\epsilon_{\parallel} = a_{\parallel}/a - 1$ appearing in Equation 1. The out-of-plane lattice constant can then be calculated using the mechanical symmetries of the face-centered cubic lattice, [19] thereby obtaining the out-of-plane uni-axial strain $\epsilon_{\perp} = a_{\perp}/a - 1$ also appearing in Equation 1. The value of the shear deformation potential, b, in the dilute nitride is not clear. Some works claim x-dependent values as large as -3.2 eV, [20, 21] while others report values around -2.4 eV for low nitrogen contents similar to a value measured for GaAs of -1.7 eV. [18] There is a high degree of variability in the reported values of b, even for GaAs, so for the sake of simplicity a typical value of -2 eV was used to calculate the dark gray line shown in Figure 3. Using the measured splittings obtained from the fits to the PL data, an estimate for the x value can then be obtained by adjusting these points onto the dark gray line as shown in Figure 3. From the highest to lowest nitrogen content, the five alloys studied here have nitrogen fractions x equal to 0.039, 0.038, 0.035, 0.031, and 0.022 (as also noted in Figure 1(b)). The principal error in determining the alloy content is not the fit to the PL spectra since the vertical error bars in δ are negligibly small. In fact the principal uncertainty is the value of b. To estimate this error, the upper edge of the gray zone in Figure 3 was calculated with $b = -2.4$ eV, and the lower edge with $b = -1.7$ eV, two outlying values for b. In this way, given the small uncertainty in δ, conservative estimates for the horizontal error bars i.e. in x, can be made by taking the minimum and maximum values of x that fall within the gray zone. The deduced alloy contents and errors are: 0.039 ± 0.005, 0.038 ± 0.006, 0.035 ± 0.006, 0.031 ± 0.005, and 0.022 ± 0.004 respectively and these are indicated in the legend of Figure 1(b). As will be seen in the following section, these values agree well with those obtained by Raman spectroscopy. The origin of the spatial variation in x is not immediately clear. However, it is known that substrate strain and temperature during growth can sensitively affect the ability to incorporate nitrogen into the GaAs lattice. [22] It is therefore likely that one or both of these factors resulted in the spatial variation in alloy content. Such a variation opens the way for the systematic study of SDR with x on a single wafer as discussed below.
The PL fitting procedure also reveals the energy range corresponding to light emission from the Bloch density-of-states rather than the Urbach tail. In Figure 2 this corresponds to the energy range clearly above the green, dotted line but below the very high energy tail where light intensities are too low to be useful. For this particular spectrum, the heavy- and light-hole intensities to be used in the analysis of the SDR and light polarizations are therefore taken only for energies ranging from approximately 1.15 eV to 1.2 eV. A similar procedure was used on all other spectra.

2.1 Raman spectroscopy

The x values determined from the PL spectra were verified by studying the N-related vibrational modes in a Raman scattering map of the wafer surface, the result of which is shown in **Figure 4(a)**. The spectra shown in Figure 4(b) exhibit a Raman peak at 470 cm^{-1} corresponding to a GaN-related (LO_2), optical phonon mode. [15] These data were taken using a 1 mW off-resonance excitation at 2.62 eV focused to a $\sigma = 1$ μm Gaussian spot. This peak increases with intensity relative to the GaAs-related optical phonon modes located between 500 cm^{-1} and 550 cm^{-1}. Using the approach introduced by Wagner, [15] a spa-

tially resolved map of nitrogen content was measured. This was achieved by removing a linear background between 430 cm^{-1} and 550 cm^{-1} which yields the spectra shown in **Figure 4(b)**. The integrated intensity of the GaN-like mode between 460 cm^{-1} and 490 cm^{-1} was then normalized to the integrated intensity of the GaAs-like modes between 500 cm^{-1} and 550 cm^{-1}. These wavenumber ranges are indicated by the shaded areas in Figure 4(b). The known linear relationship between the resulting normalized intensity and the alloy content, x, [15] was then used to determine the nitrogen content at each point on the sample, the map of which is shown in Figure 4(a).
The nitrogen content map obtained by Raman spectroscopy covers the same area of the sample used for the PL measurements as can be seen by comparing the white light images in Figure 1(a) and Figure 4(a). The black-outlined squares correspond to identical points in both cases, so the estimated x values obtained by fitting the PL, and via Raman scattering, can be directly compared. The excellent agreement between the two methods indicates that the nitrogen contents of the alloy can be determined with some confidence. This is emphasized in Figure 3 where the x values determined by Raman scattering, shown in color, align closely with the PL-determined points.

3 SDR as a function of alloy content

When the sample is excited with circularly polarized laser light, a spin polarization of conduction electrons is introduced according to the optical selection rules for allowed band-to-band transitions. This in turn results in a dynamic polarization of the paramagnetic centers associated with Ga^{2+} interstitials. In steady-state, the polarization of the centers is similar to that of the conduction electrons, [6] and according to the exchange interaction, this prevents recombination of the dominant spin species via these trap states. This in turn increases the PL intensity when switching from linearly- to circularly-polarized pump light. As previously described, the ratio of these two PL intensities is called the SDR ratio and is shown in **Figure 5(a)** for varying excitation powers and alloy contents.
For each of the studied alloys, the SDR ratio shows the characteristic peak as a function of the excitation power with the maximum ratio occurring at P_{max} where the photo-excited conduction electron density is comparable to the defect density. A qualitative explanation for this is as follows: at low excitation powers, where the photo-electron density is small compared to the density of paramagnetic defects, only a small fraction of the defects are dynamically polarized and the SDR is small. At high excitation powers, where the photo-electron density is much higher than the paramagnetic defect density, the defects progressively transit to the doubly-occupied state, which is no longer an electronically active trap state. In this case, the SDR also drops. Quantitatively, this behavior can be captured by a coupled rate equation model for the electron, hole and trap state densities, [6] but no attempt is made here to fit this model to the presented data.
In spite of this it is important to note that a measurement of P_{max} gives an indication of the relative density of SDR-active centers. The observation that P_{max} increases with increasing nitrogen content, as seen in **Figure 5(d)**, therefore suggests that the density of paramagnetic traps responsible for SDR increases with increasing nitrogen content. The importance of using extremely high excitation power densities up to $\approx 10^7$ Wcm^{-2} for PL measurements therefore becomes apparent. It allows for the full SDR ratio versus power curves to be measured, even for high nitrogen contents where SDR-active defect densities and hence P_{max} are large. Indeed, previous reports of SDR in dilute nitrides have only studied alloy contents up to $x = 0.026$, even with the use of high peak intensity pulsed excitation. [23]
Another important observation is that the maximum SDR ratio monotonically decreases with increasing nitrogen content as seen in **Figure 5(c)**. This second observation can be qualitatively explained by an increase in other, as-yet unidentified, SRH centers through which spin-independent recombination rates become comparable to, or greater than, the spin dependent recombination rate occurring via the Ga^{2+}-related centers. This increase in available non-radiative recombination routes is consistent with the monotonic decrease in PL intensity with increasing x seen in **Figure 5(b)**. This is also apparent in Figure 1(b) where the normalization factors for each spectrum are shown i.e. for $x = 0.039$ the spectrum is 18.7 times less intense than the $x = 0.022$ spectrum. These observations of the SDR and its power

dependence versus alloy content therefore clearly indicate the necessity to include non-spin-dependent recombination paths in any complete description of SDR. This conclusion has been made previously on the basis of the power dependence of the SDR for a single alloy. [16] The alloy dependence observed here reinforces this conclusion.

4 Conclusion

Spin-dependent recombination in dilute nitrides has been studied as a function of alloy content on a single wafer where a likely temperature and strain variation during growth results in a gradient in nitrogen content as a function of position. The nitrogen content of the alloys is determined to an accuracy of approximately 0.005 using two independent approaches, one based on a fit of the PL spectra using a Roosbroeck-Shockley model, and another using the relative intensity of GaN-like phonon modes in the Raman spectrum. The excellent agreement between these two methods indicates that while only strictly applicable in equilibrium i.e. to absorption spectra, the Roosbroeck-Shockley model can be applied to PL at least for sufficiently low excitation powers.
Use of excitation power densities significantly higher than those previously reported in the literature allows for the full SDR ratio versus excitation power curves to be measured, even at the highest available nitrogen content. A systematic reduction in maximum SDR ratio and in PL intensity with increasing nitrogen content, along with an associated increase in P_{max}, indicates that the density of all SRH centers, both those which yield spin-dependent *and* spin-independent recombination paths, must be accounted for in any complete physical model of SDR in these materials.

Acknowledgements
This work was supported by the Simons Foundation (grant No 601944) and by the Agence Nationale de la Recherche (grant No ANR-17-CE24-0005)

References

[1] F. Rong, W. Buchwald, E. Poindexter, W. Warren, D. Keeble, *Solid-State Electronics* **1991**, *34*, 835.

[2] Kaplan, D., Solomon, I., Mott, N.F., *J. Physique Lett.* **1978**, *39*, 51.

[3] C. Weisbuch, G. Lampel, *Solid State Communications* **1974**, *14*, 141.

[4] D. Lepine, *Phys. Rev. B* **1972**, *6*, 436.

[5] I. Solomon, D. Biegelsen, J. Knights, *Solid State Communications* **1977**, *22*, 505.

[6] V. Kalevich, E. Ivchenko, M. Afanasiev, A. Shiryaev, A. Egorov, V. Ustinov, B. Pal, Y. Masumoto, *JETP Letters* **2005**, *82*, 455.

[7] V. Kalevich, A. Shiryaev, E. Ivchenko, A. Egorov, L. Lombez, D. Lagarde, X. Marie, T. Amand, *JETP Letters* **2007**, *85*, 174.

[8] F. Zhao, A. Balocchi, A. Kunold, J. Carrey, H. Carrre, T. Amand, N. B. Abdallah, J. C. Harmand, X. Marie, *Applied Physics Letters* **2009**, *95*, 241104.

[9] X. Wang, I. Buyanova, F. Zhao, D. Lagarde, A. Balocchi, X. Marie, C. Tu, J. Harmand, W. Chen, *Nature materials* **2009**, *8*, 198.

[10] S. Chen, Y. Huang, D. Visser, S. Anand, I. Buyanova, W. Chen, *Nature Communications* **2018**, *9*, 1.

[11] R. Joshya, H. Carrère, V. Ibarra-Sierra, J. Sandoval-Santana, V. Kalevich, E. Ivchenko, X. Marie, T. Amand, A. Kunold, A. Balocchi, *Advanced Functional Materials* **2021**, *31*, 064040.

[12] V. Kalevich, A. Y. Shiryaev, E. Ivchenko, M. Afanasiev, A. Y. Egorov, Y. Ustinov, V.M.and Masumoto, *Physica B: Condensed Matter* **2009**, *404*, 4929.

[13] X. J. Wang, Y. Puttisong, C. W. Tu, A. J. Ptak, V. K. Kalevich, A. Y. Egorov, L. Geelhaar, H. Riechert, W. M. Chen, I. A. Buyanova, *Applied Physics Letters* **2009**, *95*, 241904.

[14] B. Ullrich, S. Munshi, G. Brown, *Semiconductor Science and Technology* **2007**, *22*, 1174.

[15] J. Wagner, T. Geppert, K. Köhler, P. Ganser, N. Herres, *Journal of Applied Physics* **2001**, *90*, 5027.

[16] A. Kunold, A. Balocchi, F. Zhao, T. Amand, N. B. Abdallah, J. Harmand, X. Marie, *Physical Review B* **2011**, *83*, 1.

[17] E. P. O'Reilly, A. Lindsay, P. J. Klar, A. Polimeni, M. Capizzi, *Semiconductor Science and Technology* **2009**, *24*, 033001.

[18] W. Li, M. Pessa, J. Likonen, *Applied Physics Letters* **2001**, *78*, 2864.

[19] A. Egorov, V. Kalevich, M. Afanasiev, A. Shiryaev, V. Ustinov, M. Ikezawa, Y. Masumoto, *Journal of Applied Physics* **2005**, *98*, 013539.

[20] Y. Zhang, A. Mascarenhas, H. Xin, C. Tu, *Phys. Rev. B* **2000**, *61*, 7479.

[21] T. Ikari, S. Fukushima, Y. Ohta, A. Fukuyama, S. D. Wu, F. Ishikawa, M. Kondow, *Phys. Rev. B* **2008**, *77*, 125311.

[22] M. Reason, H. A. McKay, W. Ye, S. Hanson, R. S. Goldman, V. Rotberg, *Applied Physics Letters* **2004**, *85*, 1692.

[23] F. Zhao, A. Balocchi, G. Truong, T. Amand, X. Marie, X. Wang, I. A. Buyanova, W. Chen, J. Harmand, *Journal of Physics: Condensed Matter* **2009**, *21*, 174211.

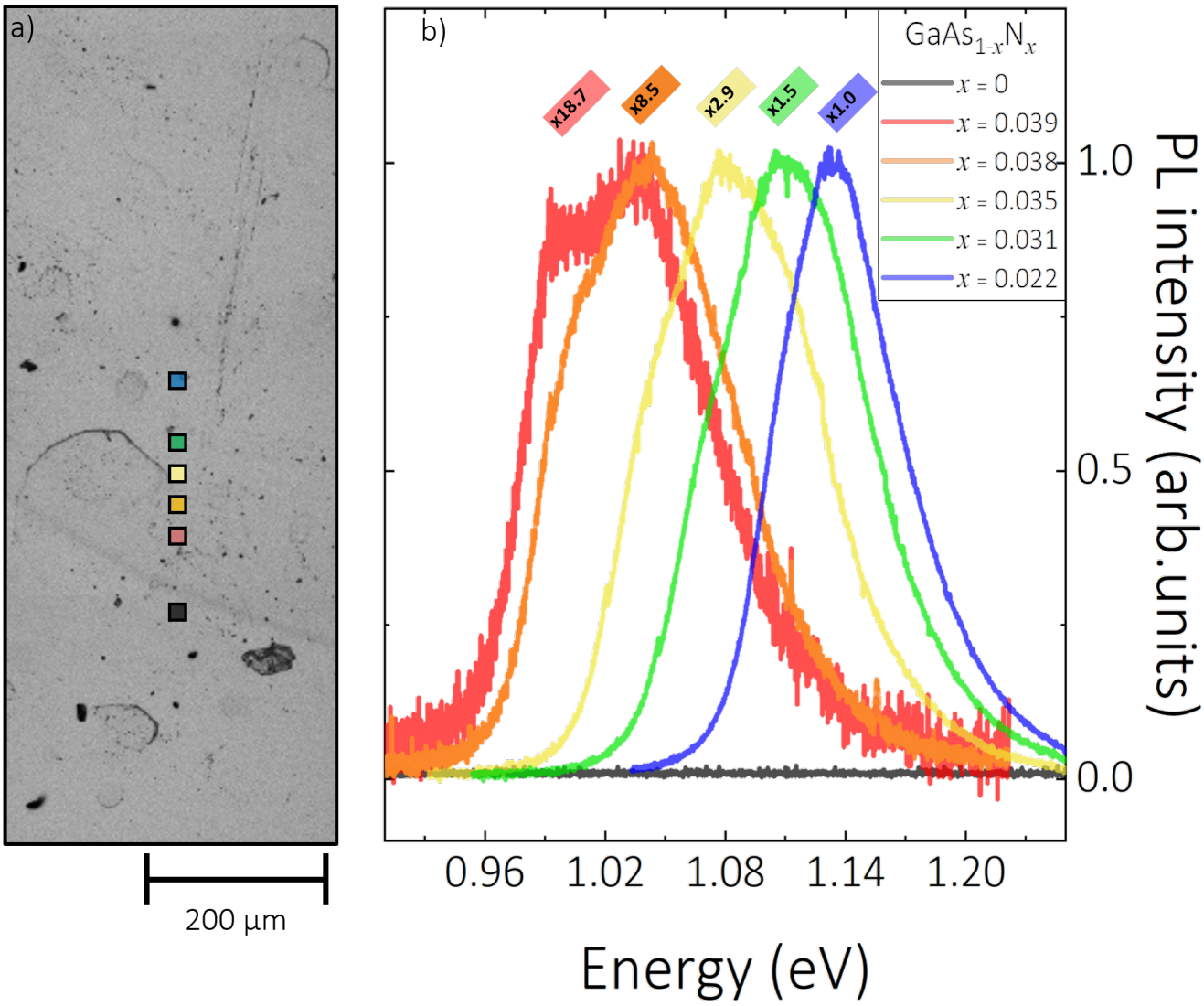

Figure 1: (a) Brightfield image of the 50 nm thick, nominal $x = 0.021$ $GaAs_{1-x}N_x$ epilayer. Areas probed by PL spectroscopy are indicated by the black-outlined squares and the corresponding spectra are shown in (b). A red shift in the PL indicates a local increase in x which is accompanied by a shear-stress-induced splitting of the PL peak into heavy- and light-hole components. The x values determined by a fit of the PL are given in the legend.

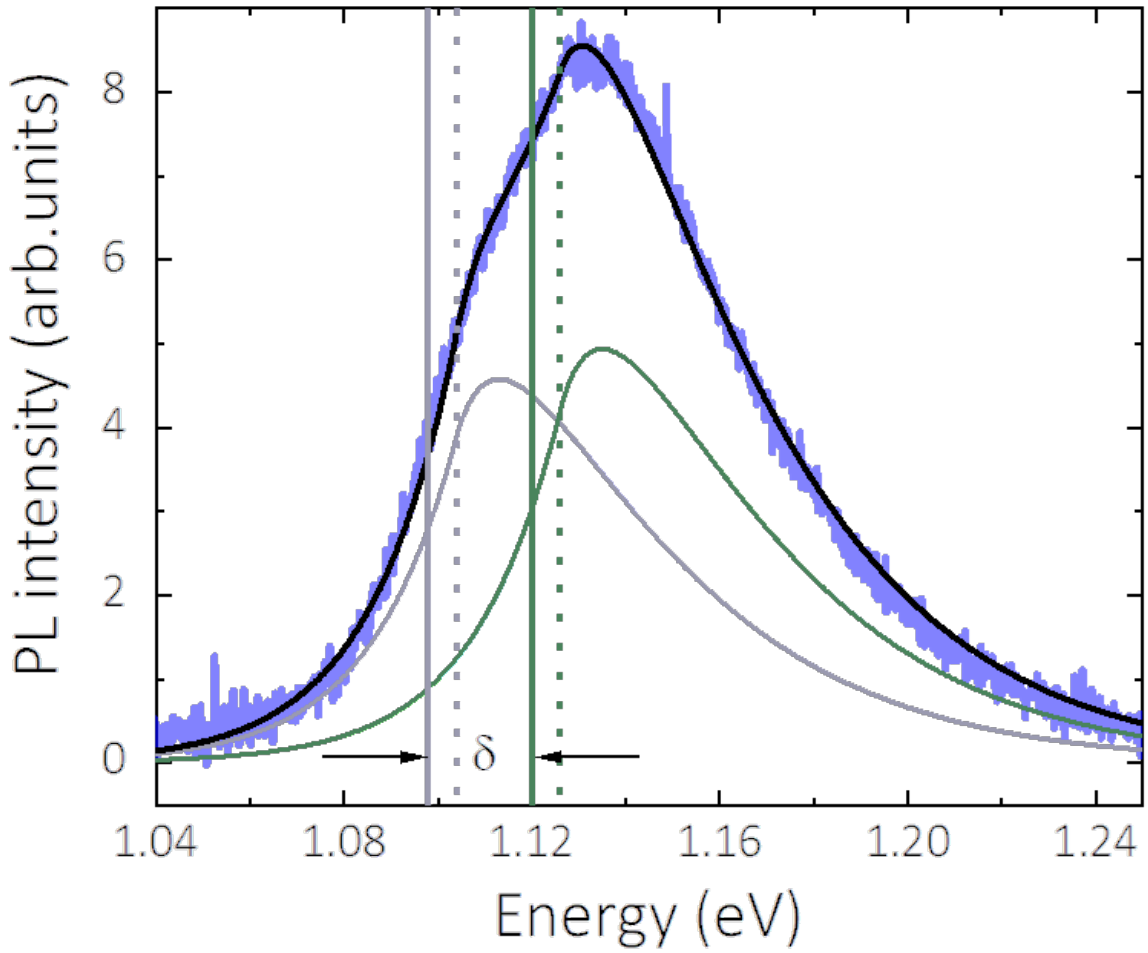

Figure 2: PL intensity under linearly polarized excitation for the x = 0.022 point on the sample surface (also shown in blue in Figure 1(a)). The fitting for light holes (gray), heavy holes (green), and the cumulative fit (black) are shown. The gap values for the light and heavy holes are highlighted with solid lines and the critical energies are denoted by dotted lines. The hole splitting energy, δ, used in Equation 1 to determine the layer strain is the difference in the gap energies as indicated.

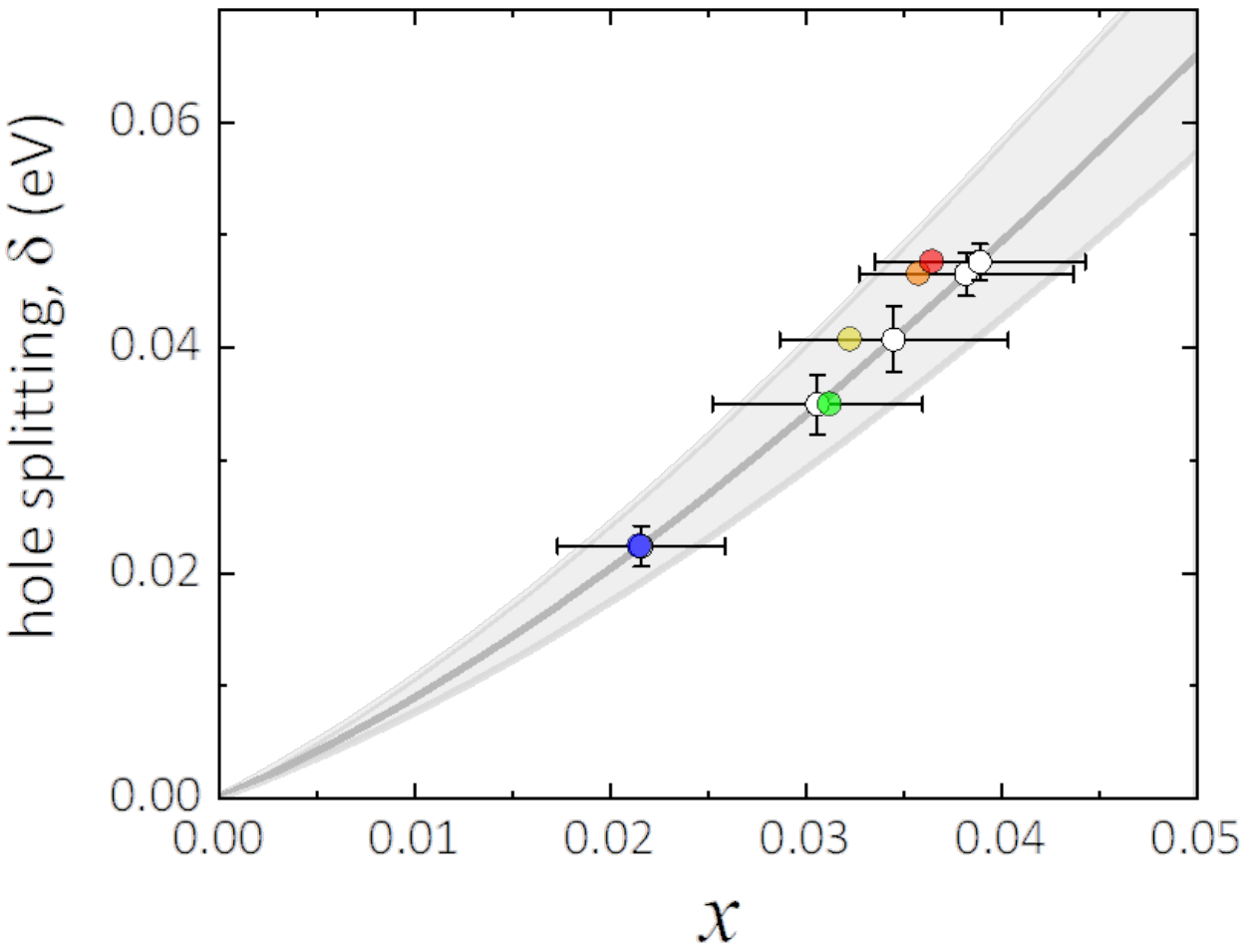

Figure 3: Hole splitting energies, δ, plotted as a function of alloy nitrogen content, x. The black line corresponds to a shear deformation potential, $b = -2$ eV in Equation 1. The upper and lower limits of values for b are indicated by the gray region. The nitrogen content of the five studied alloys is estimated by placing the measured hole splittings (open circles) on the black line. The results, obtained from the (red to blue) spectra in Figure 1(b), are 0.039 ± 0.005, 0.038 ± 0.006, 0.035 ± 0.006, 0.031 ± 0.005, and 0.022 ± 0.004. The x error is estimated by taking the maximal x between the two extreme b values corresponding to the standard error in δ (vertical error bars) found from the PL spectral fit. The colored circles correspond to the x values found using Raman spectroscopy at the same points on the sample.

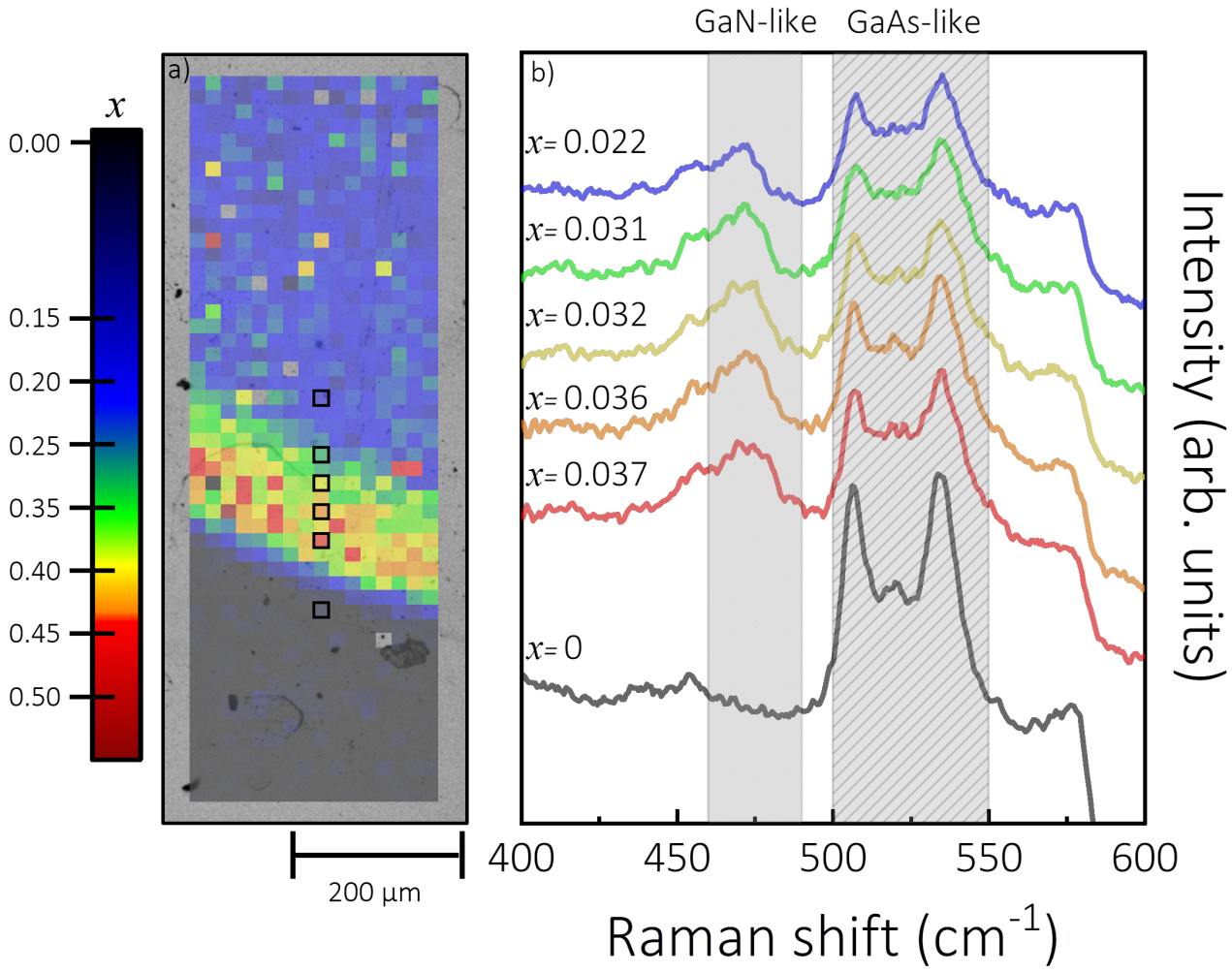

Figure 4: (a) Brightfield image of the $GaAs_{1-x}N_x$ sample with a superimposed map of the variation in x. The pixel spacing is 20 μm. Pixel values represent the x determined using Wagner's approach [15] which compares the integrated intensity of the GaN-like LO_2 phonon (460 - 490 cm^{-1}) to that of the GaAs-like second order phonon spectrum (500 - 550 cm^{-1}). The resulting extremes of nitrogen content on the wafer range from $x = 0$ to $x = 0.045$. Representative spectra are shown in (b) and are labeled with corresponding x values taken from the black-outlined pixels in (a).

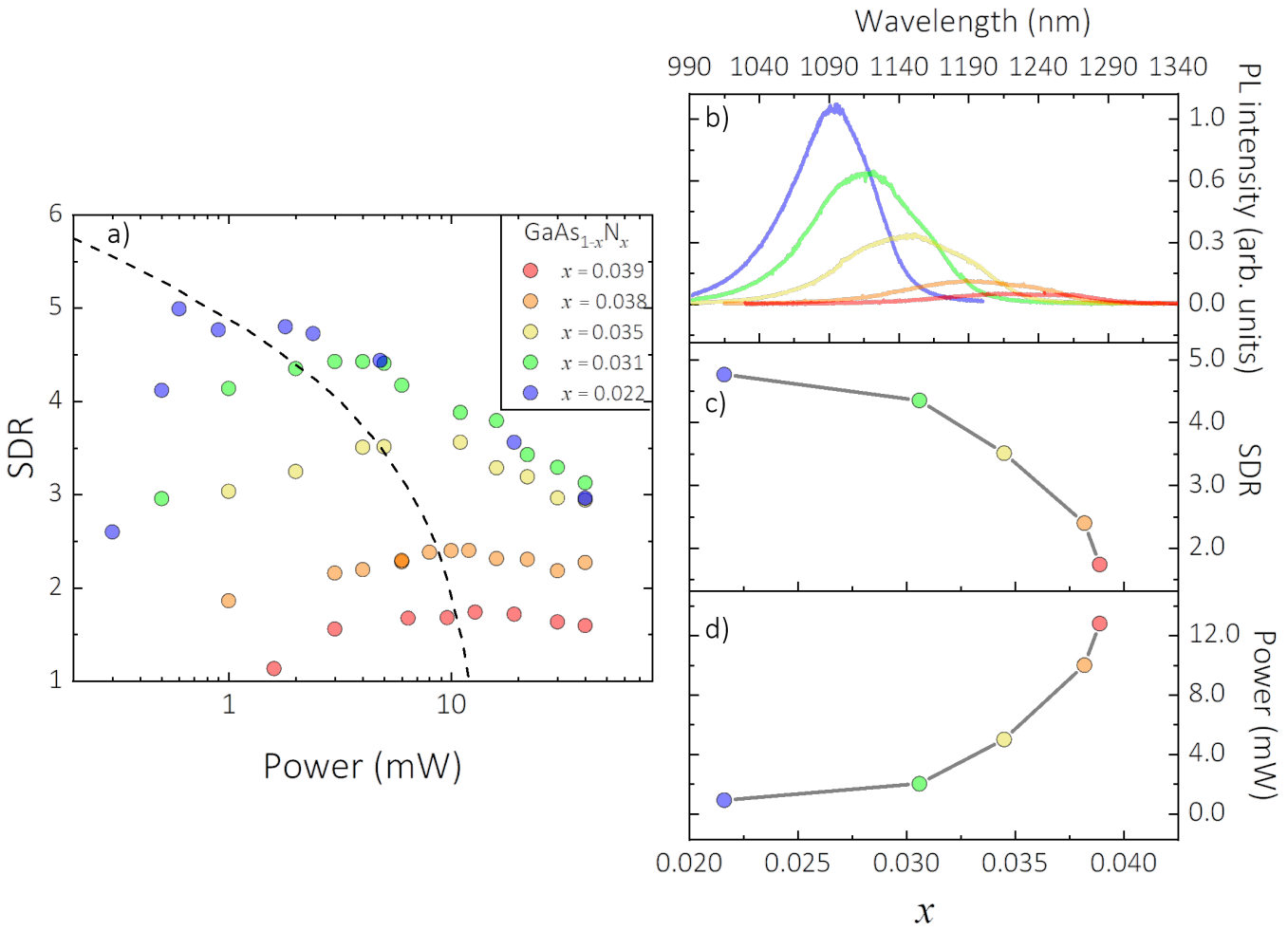

Figure 5: (a) SDR as a function of excitation power for different nitrogen contents. A dashed line gives a guide to the eye describing the power at which peak SDR occurs for the different x values, $P_{\max}$. This variation is also shown in (d) while the corresponding SDR values are shown in (c). The decrease in PL intensity with increasing x which was already apparent in Figure 1(a) , is explicitly shown in (b)

Table of Contents

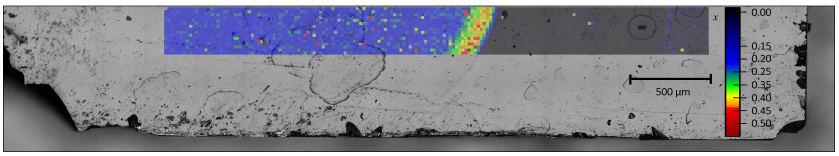

Spatial variations of nitrogen content on the surface of a dilute nitride. A systematic study of spin-dependent recombination as a function of x in dilute nitrides of the form $GaAs_{1-x}N_x$ reveals that any complete model of the phenomenon must also include spin-independent Shockley-Read-Hall recombination paths.